Alternatively spliced proline-rich cassettes link WNK1 to aldosterone action

Supplemental Data and Methods

Ankita Roy[1], Lama Al-Qusairi[2], Bridget F. Donnelly[1], Caroline Ronzaud[2], Allison L. Marciszyn[1], Fan Gong[1], Y.P. Christy Chang[3], Michael B. Butterworth[4], Núria M. Pastor-Soler[1,4], Kenneth R. Hallows[1,4], Olivier Staub[2], and Arohan R. Subramanya[1,4,5]

[1]Departments of Medicine, University of Pittsburgh School of Medicine, Pittsburgh, Pennsylvania, USA; [2]Department of Pharmacology and Toxicology, University of Lausanne, Lausanne, Switzerland; [3]Department of Medicine, University of Maryland Medical School, Baltimore, Maryland, USA; [4]Department of Cell Biology, University of Pittsburgh School of Medicine, Pittsburgh, Pennsylvania, USA; [5]VA Pittsburgh Healthcare System, Pittsburgh Pennsylvania, USA

Contact:
Arohan R. Subramanya, MD
Department of Medicine, Renal-Electrolyte Division
University of Pittsburgh School of Medicine
S828A Scaife Hall
3550 Terrace Street
Pittsburgh, PA 15261
Tel 412.624.3669 Fax: 412.647.6222
Email: ars129@pitt.edu

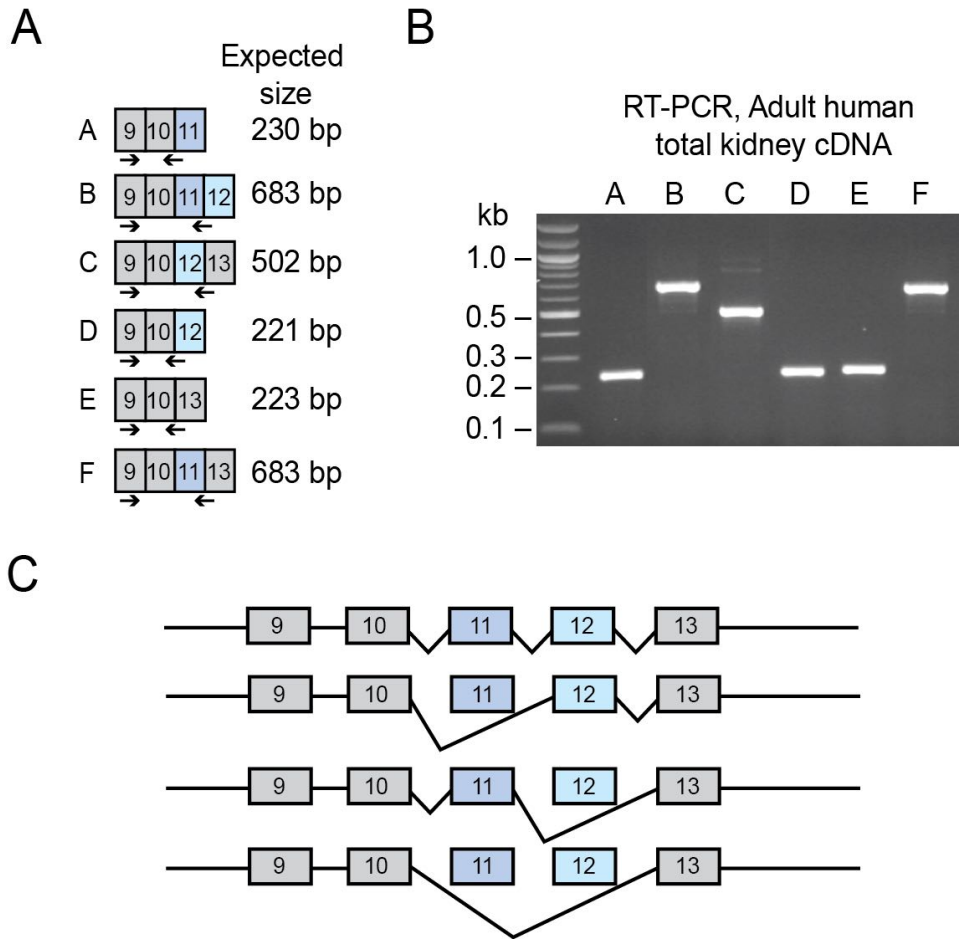

Figure S1. Exons 11 and 12 undergo extensive alternative splicing in human kidney.

(A.) RT-PCR reactions were performed, using a forward primer that binds to exon 9 and reverse primers designed to anneal to exon junctions 10/11, 11/12, 12/13, 10/12, 10/13, and 11/13 (see Table S1). Annealing sites for the forward and reverse primers set are depicted with arrows, and the predicted amplicon size for each RT-PCR product is listed next to each isoform.

(B.) Agarose gel electrophoresis of RT-PCR products from human kidney RNA. The PCR products in rows A-F of the gel were generated using primer sets corresponding to isoforms A-F in panel A. Representative of 2 experiments.

(C.) Schematic representation of all WNK1 splicing events occurring between exons 10 and 13 identified in human kidney. These data are consistent with previously published observations (1, 2).

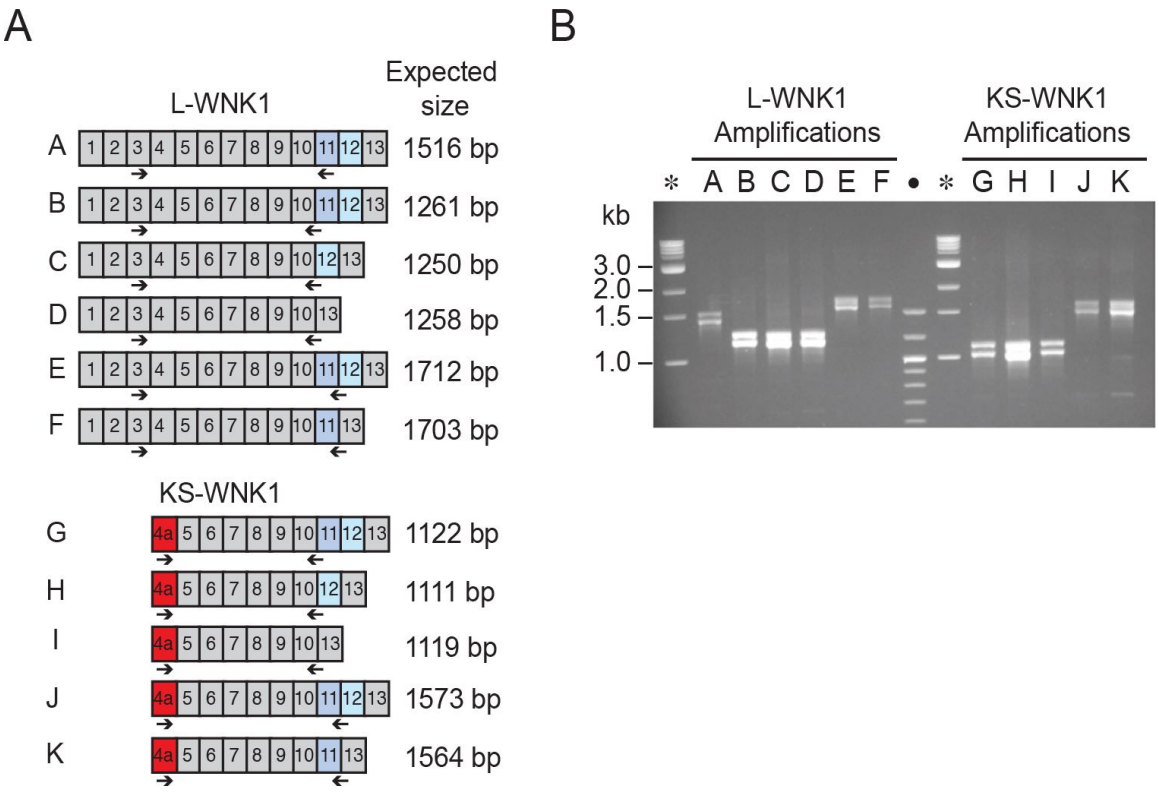

Figure S2. L-WNK1 and KS-WNK1 contain a complete assortment of exon 11 and 12 combinations.

(A.) RT-PCR reactions were performed on adult human kidney RNA using methods similar to those in Figure S1. For these reactions, forward primers specific for L-WNK1 (exon 3) and KS-WNK1 (exon 4a) were used in combination with reverse primers designed to anneal to exon junctions 10/11, 11/12, 12/13, 10/12, 10/13, and 11/13 (see Table S1). Annealing sites for these primers are depicted with arrows, and predicted amplicons sizes are listed next to each isoform.

(B.) Agarose gel electrophoresis of RT-PCR products from human kidney RNA. The PCR products in rows A-K of the gel were generated using primer sets corresponding to isoforms A-K in panel A. 1kb and 100bp ladders (New England Biolabs) are indicated with *asterisks* and a *dot*, respectively. In each case, a doublet was identified, and sequencing of the shorter major band identified additional alternative splicing events in exon 9. These data match the findings of a recent report (3). Representative of 2 experiments.

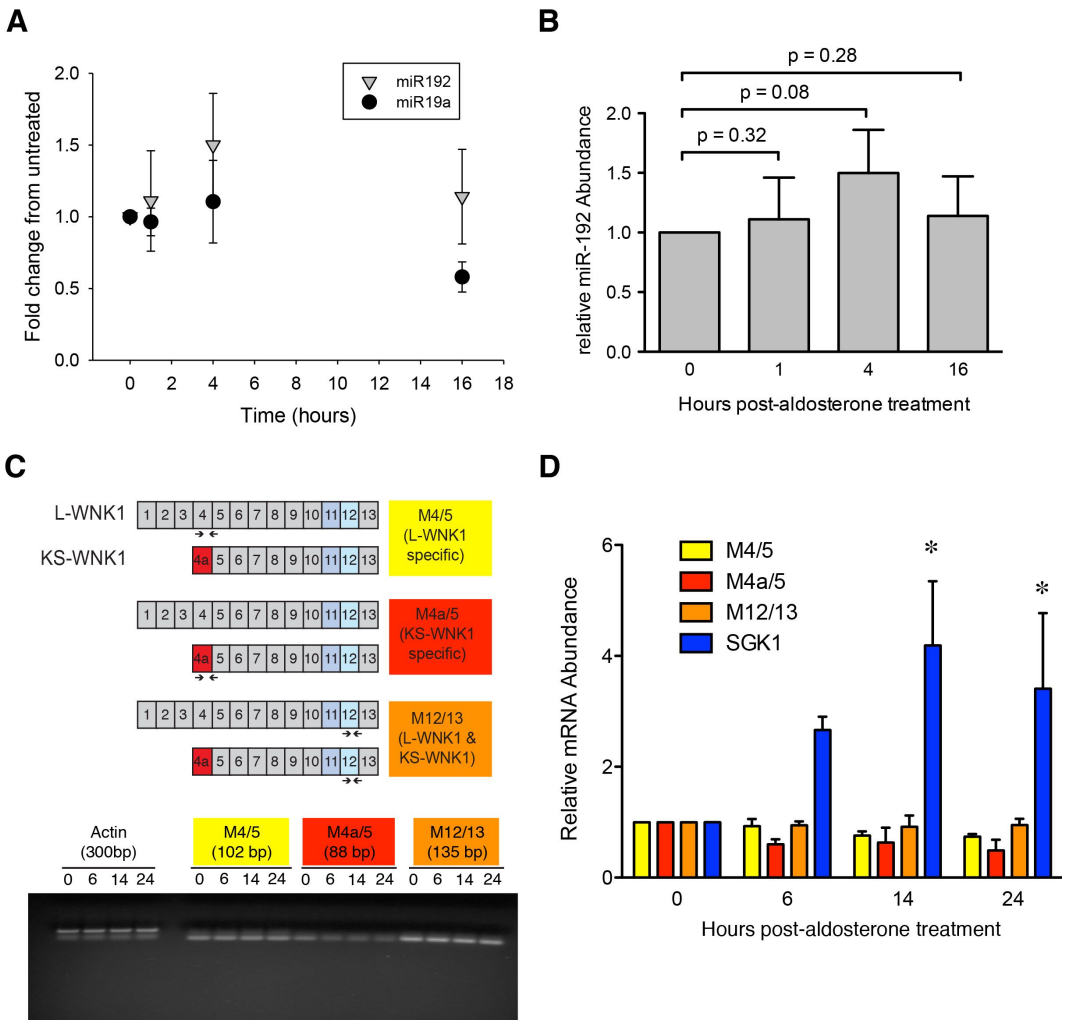

Figure S3. WNK1 transcript abundance is not increased by 100nM aldosterone in mpkCCD$_{c14}$ cells.

(A.) mpkCCD$_{c14}$ cells were treated with 100nM aldosterone for up to 16h, and miR-192 abundance was assessed by quantitative real-time PCR (qRT-PCR) using the SYBR-green intercalation method. Parallel quantitative analysis of miR-19a, a control microRNA that is not affected by aldosterone, was also performed. miRNA abundance at each time point was normalized to the abundance at time zero. (B.) Quantification of miR-192 abundance following 1, 4, and 16h aldosterone treatment, normalized to the abundance at time zero. P values reflect standard unpaired T-test comparisons to the zero hour time point. (C.) *Top*, Schematic showing the location of primer set specific for L-WNK1 (M4/5), KS-WNK1 (M4a/5) and Exon 12 (M12/13) WNK1 isoforms, indicated with arrows. *Bottom*, Representative PCR reactions demonstrating single WNK1 amplicons of expected size, using the indicated primer sets, during a 24h 100nM aldosterone timecourse. (D.) Quantification of WNK1 isoform abundance following 6, 14, and 24h of 100nM treatment. An increase in SGK1 transcription was detected, indicating that the cells were aldo responsive. (n=4; *P<0.05 vs the zero time point by Kruskal-Wallis test with Dunn's multiple comparison post-hoc test).

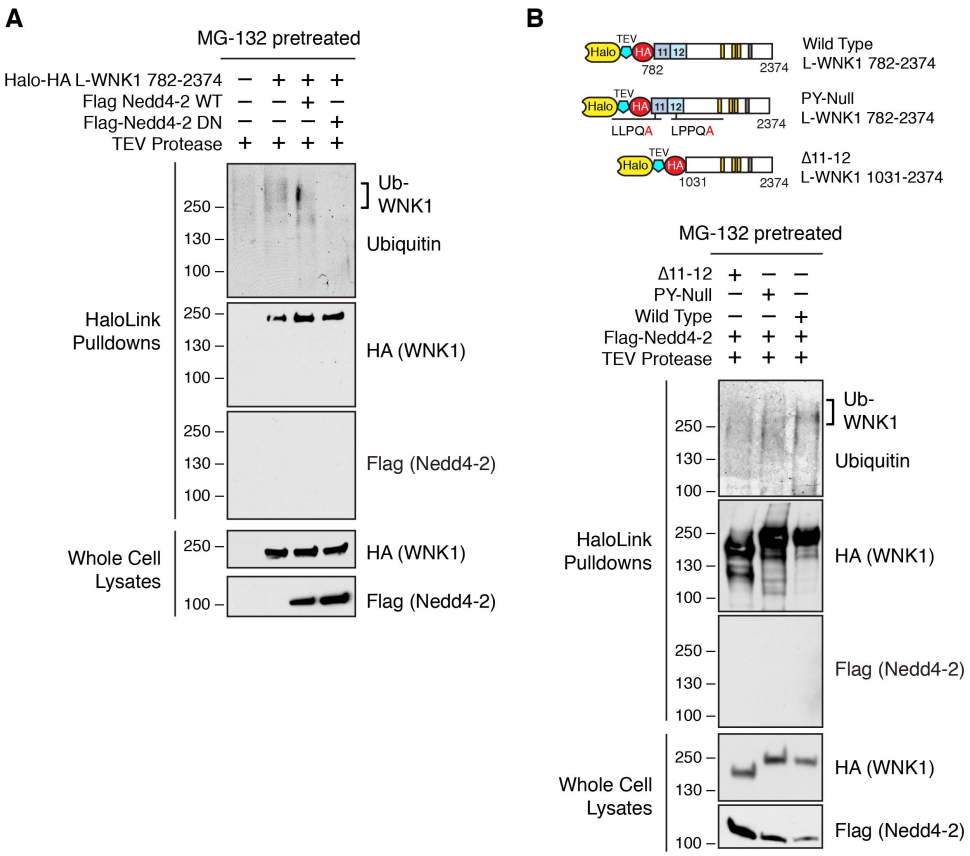

Figure S4. Nedd4-2 mediated ubiquitylation of the WNK1 C-terminus is PY-motif-dependent and requires intact catalytic activity.

(A.) In vivo ubiquitylation assay of Halo-HA-L-WNK1 C-terminus containing exons 11 and 12 (L-WNK1 782-2374). Lysates of MG-132 pretreated HEK-293T cells expressing WNK1 fragments with WT or catalytically inactive dominant negative (DN; C938S) Nedd4-2 were covalently attached to HaloLink resin. Following pulldown, fragments were washed with SDS to remove autoubiquitylated Nedd4-2 and other ubiquitylated co-precipitants. The fragments were then cleaved from the resin with TEV protease and probed with the indicated antibodies. A stronger immunoreactive smear is noted when L-WNK1 is coexpressed with Nedd4-2; this smear is absent in samples where L-WNK1 is coexpressed with DN Nedd4-2. Representative of 4 experiments. (B.) *Top*, Schematic representation of C-terminal Halo HA-tagged constructs used for the experiments: Wild type C-terminus containing exons 11 and 12, a "PY-null" mutant lacking Nedd4-2 binding sites, and L-WNK1 1031-2374, a construct encoding exon 13 to the C-terminal end of the protein ("Δ11-12"). *Bottom*, the above constructs were coexpressed with WT Nedd4-2 in HEK-293T cells and subjected to the ubiquitylation assay following MG-132 pretreatment. A stronger immunoreactive smear was observed with the "Wild Type" L-WNK1 C-terminus, compared to the double PY motif mutant or the Δ11-12 construct. Representative of 3 experiments.

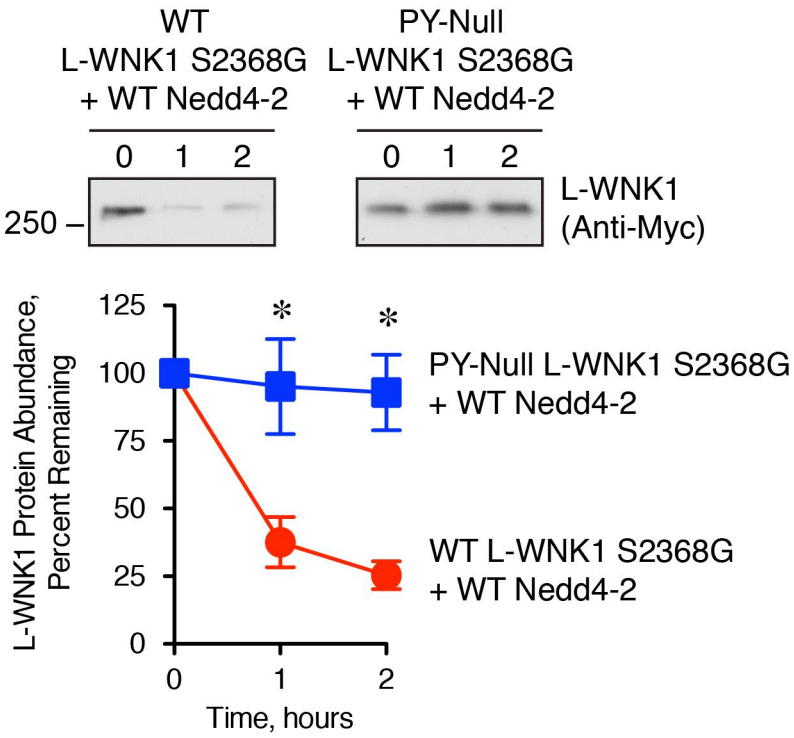

Figure S5. Variant serine at residue 2368 of L-WNK1 does not influence Nedd4-2 sensitivity.

A variant serine at the C-terminal end of the original L-WNK1 clone (AAF74258.1) that replaces a phylogenetically conserved glycine residue was recently reported to confer reduced L-WNK1 activity toward NCC (4). This residue (serine 2368 based on the numeration for RefSeq XP_008761429.1, corresponding to the full length rat L-WNK1 amino acid sequence encoded by the cDNA construct used for these studies) was mutated back to the conserved glycine in both WT and PY-Null (Y829A/Y945A) L-WNK1 constructs. Cycloheximide chases were then performed as outlined in the Methods. (n=4; *P<0.01 by Student's T-tests for the indicated time points).

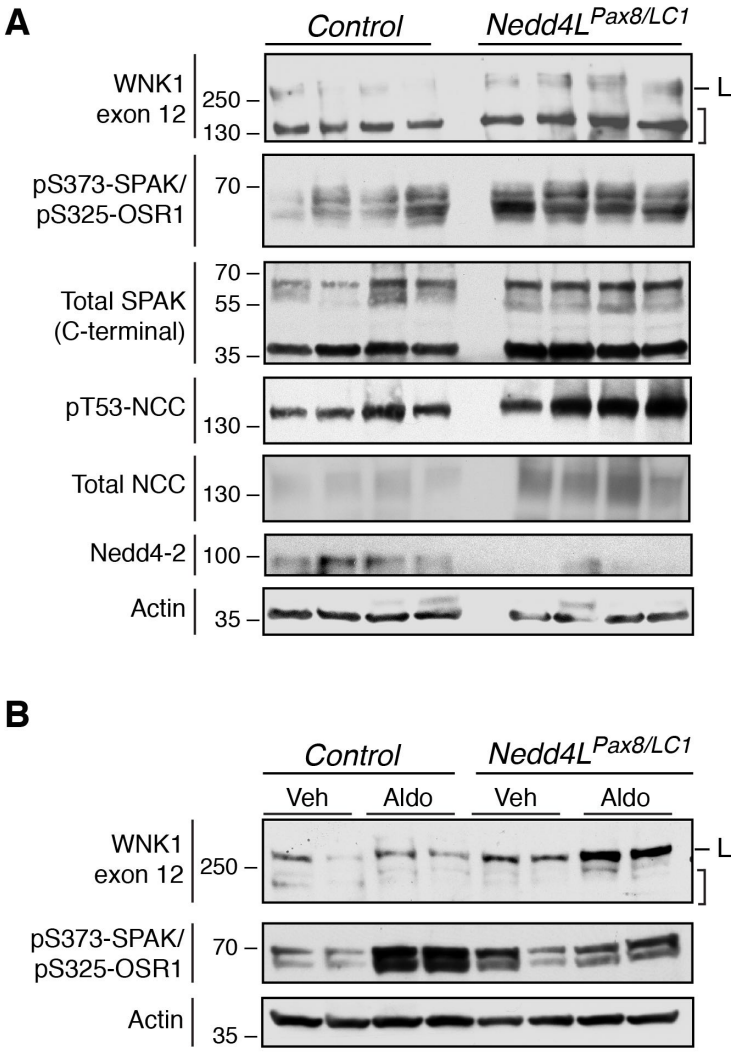

Figure S6. Additional immunoblots comparing control and Nedd4-2$^{Pax8/LC1}$ mice.

(A.) WNK1 exon 12, SPAK/OSR1, and NCC abundance in kidney homogenates from Nedd4-2$^{Pax8/LC1}$ mice and single transgenic controls treated with high salt diet. (B.) WNK1 exon 12 and phospho-SPAK abundance in Nedd4-2 knockouts and single transgenic controls treated with 3d of aldosterone of vehicle by subcutaneous osmotic minipump. In both exon 12 blots, full length L-WNK1 ("L") and lower molecular weight species (brackets) are shown. In the blot for (B), the membrane was cut above ~150kDa. Control values were normalized to a mean of 100%, and densitometry values from Nedd4-2$^{Pax8/LC1}$ mice were expressed relative to the mean of the control. Actin-normalized data were pooled with the immunoblotting studies in Fig 9.

Table S1. Oligonucleotide sequences used in the study.

cloning of exons 11 & 12 from rat kidney cDNA		
rWNK1ex10_Age1.FOR rWNK1ex14_Sal1.REV	gttctatcttcacaaccggtccaacatcctcagca ctgaatgggcactgtcgacagaggaaaccaatg	
mutagenesis oligos for PY motif deficient construct (exon 12 PY motif)		
rWNK1ppqy_ppqa.FOR rWNK1ppqy_ppqa.REV	ccatctcgactgccaccacaagccccaggagattcaaata tatttgaatctcctggggcttgtggtggcagtcgagatgg	
mutagenesis oligos for PY motif deficient construct (exon 11 PY motif)		
rWNK1llpqy_llpqa.FOR rWNK1llpqy_llpqa.REV	cctacttctttactcccacaggctcctgtctctcaaatttccat atggaaatttgagagacaggagcctgtgggagtaaagaagtagg	
mutagenesis oligos for S2368G construct		
rLWNK1S2368G.FOR rLWNK1S2368G.REV	tcagcaacccccaggttccaacctacgg ccgtaggttggaacctgggggttgctga	
oligos for RT-PCR of WNK1 isoforms from human kidney RNA		
hWNK1E3F	ggcttcttttgccaagagtg	Exon 3 forward primer (L-WNK1 specific)
hWNK1E4aF	aattctcattgctgctgctg	Exon 4a forward primer (KS-WNK1 specific)
hWNK1E9F	gggtcagccatcctcaagta	Exon 9 forward primer
hWNK1E11_13R	gagtactctggtacagaacatctcca	Exon 11/13 junction reverse primer
hWNK1E11_12R	ggaagccctggtacagaaca	Exon 11/12 junction reverse primer
hWNK1E10_13R	tccctgagtactctgttttccag	Exon 10/13 junction reverse primer
hWNK1E10_12R	agccctgttttccagctgat	Exon 10/12 junction reverse primer
hWNK1E10_11R	ctgggaaactggaagctgtt	Exon 10/11 junction reverse primer
oligos for WNK1 transcript measurements in mpkCCDc14 cells		
m4.FOR	gggatgtgcatgcttgagatggc	Exon 4 forward primer (L-WNK1 specific)
m4/5.REV	gcttcactccactggtcactc	Exon 4/5 junction reverse primer (L-WNK1)
m4a.FOR	gaagaaagatttttgttcag	Exon 4a forward primer (KS-WNK1 specific)
m4a/5.REV	cttcactccctcatttatac	Exon 4a/5 junction reverse primer (KS)
m12.FOR	caactcctttggttcctatgggc	Exon 12 forward primer
m12/13.REV	ctccctgagtactctccagaac	Exon 12/13 junction reverse primer
SGK1 Forward	ctgctcgaagcacccttacc	SGK1 positive control
SGK1 Reverse	tcctgaggatgggacattttca	SGK1 positive control
Actin Forward	gcagctccttcgttgccggt	
Actin Reverse	ggggccacacgcagctcatt	
oligos for microRNA studies in mpkCCDc14 cells		
mmu-miR-19a	tgtgcaaatctatgcaaaactga	miR-19a specific
mmu-miR-192	ctgacctatgaattgacagcc	miR-192 specific
snoRNA-135	gtagtggtgagcctatggttttctg	small nucleolar RNA control
snoRNA-202	gtacttttgaaccctttccatctg	small nucleolar RNA control

Supplemental Methods

Molecular Methods

All L-WNK1 clones used in this study were derived from the original rat L-WNK1 cDNA, isolated from rat forebrain by Xu et al (AAF74258.1, (5)). This cDNA encodes a splice isoform that lacks exons 11 and 12, and is termed "L-WNK1 Δ11-12" in this study. Site directed mutagenesis (QuickChange XL kit, Agilent) was performed to introduce silent *AgeI* and *SalI* restriction sites in exons 10 and 14 of pGH19-KS-WNK1 (6), respectively. Primers containing *AgeI* and *SalI* restriction sites were then used to amplify corresponding regions spanning exons 10-14 from a rat kidney cDNA library (Clontech) by PCR (Phusion, New England Biolabs). A 930bp fragment containing exons 11 and 12 was ligated to the *AgeI* and *SalI* sites of pGH19-KS-WNK1. A *PacI-XbaI* fragment containing exons 11 and 12 was then swapped with the corresponding 3' end of N-terminally Myc-tagged L-WNK1 Δ11-12 in pcDNA3.1 to generate full-length Myc-L-WNK1. "PY Motif-null" (Y829A/Y945A) Myc-L-WNK1 was generated by two rounds of site-directed mutagenesis in pGH19-KS-WNK1, followed by swapping of the mutant *PacI-XbaI* fragment with the 3' end of wild-type full-length Myc-L-WNK1 in pcDNA3.1. Testing of the variant serine in the AAF74258.1 L-WNK1 clone at residue 2368 was performed by mutating the residue to glycine using site-directed mutagenesis in pgh19-KS-WNK1, and swapping a 3' *ClaI-XbaI* fragment with the corresponding 3' ends in full-length and PY Motif-null L-WNK1 in pcDNA3.1. Myc-L-WNK1 1-1030 and Myc-L-WNK1 1-782 were generated by PCR, using the full length Myc-L-WNK1 isoform as template. N-terminal hemagglutinin (HA)-tagged full-length L-WNK1, HA-L-WNK1 1-

1030, and HA-L-WNK1 782-2374 were also generated by PCR and subcloning. Halo-HA tagged L-WNK1 constructs were generated by PCR amplification of a fragment encoding the Halo tag and downstream TEV protease cleavage site, located 5' to the polylinker in pHTN HaloTag CMV-neo (Promega); this product was ligated in-frame and immediately 5' to the previously generated HA tagged L-WNK1 fragments. Flag-tagged wild-type Nedd4-2 and dominant-negative Nedd4-2 (C938S) were described previously (7). SGK1 constructs were provided by Alan Pao (Stanford School of Medicine, Stanford, CA). All sequences were completely verified using automated DNA sequence analysis performed at the University of Pittsburgh Genomics and Proteomics Core Laboratories (GPCL) prior to use. Primer sequences used for mutagenesis, cloning, and PCR-based amplification are listed in Table S1.

Antibodies and Reagents

The WNK1 exon 12 antisera were generated by immunizing rabbits to a keyhole limpet hemocyanin-conjugated peptide epitope located within exon 12 of rat WNK1 (SQPAVSLSQQPPTTSSQQC). Peptide synthesis, production of rabbit antisera, and peptide affinity purification were performed by Abgent. Commercial antibodies used in the study were: mouse monoclonal anti-myc (4A6; Millipore), mouse monoclonal anti-HA (HA-11; Covance), mouse monoclonal anti-Flag (M2; Sigma), mouse monoclonal anti-β-Actin (AC-15; Sigma), rabbit polyclonal anti-α-Tubulin (SAB3501072; Sigma), mouse monoclonal anti-Ubiquitin (P4D1; Santa Cruz), rabbit polyclonal anti-C terminal WNK1 (exon 28; SAB1300464, Sigma), rabbit polyclonal anti-N terminal WNK1 (exon 1; SAB4502802, Sigma), rabbit polyclonal anti-WNK2 (ab28852; Abcam (8)), rabbit polyclonal anti-WNK3 (07-2262; Millipore (8)), rabbit polyclonal anti-Nedd4 (07-049;

WW2 domain targeting both Nedd4-1 and Nedd4-2; Millipore), rabbit polyclonal anti-Nedd4-2 (ab46521; Abcam); rabbit polyclonal anti-phospho Nedd4-2 S328 (ab95399; Abcam), rabbit polyclonal anti-SPAK (#2281 C-terminal; Cell Signaling Technology), rabbit polyclonal anti-phospho S373 SPAK/S325 OSR1 (07-2273, "S motif"; Millipore), rabbit polyclonal anti-WNK4 (NB600-284; Novus Biologicals (8, 9)), rabbit polyclonal anti-SGK1 (#07-315, Millipore), goat anti-AQP2 (C-17, Santa Cruz). Secondary antibodies raised in goat or donkey (AQP2 immunostaining only) were from Jackson ImmunoResearch. Rabbit polyclonal anti-NCC and rabbit polyclonal anti-phospho NCC (T53) were gifts of David Ellison (Oregon Health and Science University, Portland, OR) (10, 11). Guinea pig anti-NCC was a gift from Jim Wade (University of Maryland Medical School, Baltimore, MD) (12). GSK650394 was purchased from Tocris, and LY294002 was purchased from Cell Signaling Technologies. Protein A/G beads and anti-Myc conjugated agarose resin (4A6) were purchased from Millipore. HaloLink resin and ProTEV Plus protease were purchased from Promega. All other reagents were purchased from Sigma.

RNA interference studies

ON-TARGETplus SMARTpool siRNAs [cat# L-007178-00-0005] were used to knockdown Nedd4 isoforms in HEK-293T cells. The four pooled siRNA duplexes were directed against both Nedd4-1 and Nedd4-2. Cells were transfected with 100nM siRNA using Lipofectamine 2000 as per manufacturers' recommendations. Cells were re-transfected after 48h with siRNA. 48h after the second transfection, cells were harvested, lysed and analyzed by immunoblot analysis. Scrambled non-targeting siRNA (Stealth Select RNAi negative control, Invitrogen) was used as control.

In vivo ubiquitylation assay

Cells transiently expressing the indicated constructs were pretreated 24h post-transfection with 10μM MG-132 for 4h prior to cell lysis. A total of 0.75-1.5mg of the lysate was diluted to 300μl and used in the pulldown assay. The lysates were rotated overnight at 4°C in 50μl aliquots of HaloLink resin (Promega) that had been prewashed three times in binding buffer (100mM Tris, pH 7.6, 150 mM NaCl and 0.05% IGEPAL CA-630). To remove co-precipitated proteins, the samples were centrifuged at low speed, and the beads were stringently washed three times in PBS containing 0.01% SDS and two times in PBS. Following the final wash, the resin was resuspended in 20 μl of 1X ProTEV Buffer supplemented with 1mM DTT and 30 units of ProTEV Plus Protease (Promega). The samples were incubated for two hours at 30^{o}C, shaking the beads every 10 minutes. Following the TEV digest, the beads were pelleted by low speed centrifugation. The supernatant was removed and incubated with Laemmli buffer at room temperature for 20 minutes. Samples were separated by SDS-PAGE, and analyzed by immunoblotting as described above. For the anti-ubiquitin immunoblots, following transfer to nitrocellulose, the membranes were boiled in distilled water for 10min and cooled to room temperature prior to the blocking step to expose ubiquitin moieties.

Immunoprecipitation studies

For coimmunoprecipitation studies in HEK-293T cells, cells transiently expressing the indicated constructs were lysed in detergent solution (13) as described above. 500μg lysate was diluted in detergent solution to a volume of 500μl and precleared with 50μl of Sepharose CL-6B slurry by end over end rotation at 4°C for 2 h.

The cleared lysates were rotated in fresh 25µl aliquots of anti-myc-conjugated agarose resin (Millipore, clone 4A6) overnight at 4 °C. Samples were centrifuged at low speed, and the beads were washed five times in 500µl of PBS supplemented with protease inhibitors. Immunoprecipitated proteins were eluted by incubating the beads at 90°C for 5 min in 5X Laemmli buffer, separated by SDS-PAGE, and analyzed by immunoblotting. For coimmunoprecipitation of endogenous proteins in mpkCCD$_{c14}$ cells, 500µg detergent solution-solubilized lysates were diluted to 500µl and precleared using 30µl of protein A/G beads mixed by rotation for 1hr at 4°C. Following low-speed centrifugation, 1µg of rabbit anti-Nedd4 antibody and 35µl of prewashed protein A/G beads was added to the supernatants and rotated overnight at 4°C. The samples were then centrifuged at 3000 x g, and the beads were washed three times for 5 minutes in 500µl PBS supplemented with protease inhibitors. Complexes were eluted from the beads with 5X Laemmli buffer by heating the samples at 90˚C for 5 min, and the samples were subsequently analyzed by immunoblotting.

Reverse Transcriptase PCR (RT-PCR) studies in human kidney

Total adult kidney RNA was purchased from Clontech (Cat #636584). RNA was treated with DNAse I, amplification grade (Life Technologies) and reverse-transcribed using oligodT primers and the Superscript III First-Strand Synthesis Supermix (Life Technologies). Detection of WNK1 transcripts was performed using exon-exon junction specific primers (Supplemental Table 1) and standard PCR conditions.

RNA Isolation and qRT-PCR Analysis

RNA from cultured mpkCCD$_{c14}$ cells was isolated using the miRNeasy RNA isolation kit (Qiagen) according to the manufacturer's protocol. The kit facilitated isolation of both miRNA and total RNA from each sample for use in qRT-PCR and RT-PCR. Total RNA (containing miRNAs) concentration and quality was evaluated for inclusion in subsequent in vitro transcription assays based on a spectrophotometric absorption ratio of 260/280 >1.8. For quantitative RT-PCR the nCode Express SYBR-Green miRNA with ROX qRT-PCR kit was used for reverse transcriptase and first-strand DNA synthesis for the miRNA and SuperScript VILO kit for mRNA (Invitrogen). For miRNA qRT-PCRs the miRNA-specific forward primers were paired to a universal reverse primer per the manufacture's protocol, and primer pairs were used as listed in Table S1 for mRNA qRT-PCR. Real-time PCR was carried out using an Applied Biosystems 7900HT Fast Real-Time PCR System (Life Technologies). Detected signals from miR amplifications were normalized to the relative expression of small nucleolar RNA (SNO-202 and SNO-135) or actin for mRNA, with each reaction/sample run in triplicate. Negative controls included no template and no primer omissions. Relative expression is presented as a fold change from control untreated samples (ΔΔCT). Forward primers for the mRNAs and miRNAs are listed in Table S1.

Kinase Inhibitor assays in mpkCCD$_{c14}$ cells

Hormone deprived mpkCCD$_{c14}$ cells were treated with 10μM GSK650394, a SGK1 specific inhibitor, 50μM LY294002, a P13K inhibitor, for 2 hours prior to a 5h treatment with 100nM aldosterone. Control samples were treated with DMSO for 2h prior to aldosterone treatment. Cells were pelleted, lysed and analyzed by immunoblotting.

Animal Studies

(Nedd4-2$^{Pax8/LC1}$) and single transgenic control mice (Nedd4-2^{Pax8} and Nedd4-2LC1) were treated with doxycycline (2mg/ml in drinking water containing 20% sucrose) for 11 days to induce Nedd4-2 gene ablation. Control and knockout animals were then fed with high salt diet (>3.2%Na^+) for 8 days, after which their kidneys were dissected for biochemical analysis (14). For aldosterone infusion studies, single transgenic control and Nedd4-2$^{Pax8/LC1}$ mice were given doxycycline for 12d as described above. Alzet 1003D osmotic minipumps loaded with DMSO vehicle or aldosterone (150μg/kg body weight/d) were implanted subcutaneously in control and Nedd4-2 knockout animals. Mice were sacrificed by cervical dislocation 3d post-implantation. During the infusion, the animals were maintained on a low-Na+ diet (<0.1%) to avoid aldosterone escape, as described previously (14). For studies in inducible tubule-specific SGK1 knockout mice, control (SGK1^{Pax8} or SGK1^{LC1}) and mutant (SGK1$^{Pax8/LC1}$) mice were treated with doxycycline for 12d, and placed on a low NaCl diet (<0.1%) for 7d with free access to water, then sacrificed for analysis.

Supplemental References

1. O'Reilly, M., Marshall, E., Speirs, H.J., and Brown, R.W. 2003. WNK1, a gene within a novel blood pressure control pathway, tissue-specifically generates radically different isoforms with and without a kinase domain. *J Am Soc Nephrol* 14:2447-2456.
2. Delaloy, C., Lu, J., Houot, A.M., Disse-Nicodeme, S., Gasc, J.M., Corvol, P., and Jeunemaitre, X. 2003. Multiple promoters in the WNK1 gene: one controls expression of a kidney-specific kinase-defective isoform. *Mol Cell Biol* 23:9208-9221.
3. Vidal-Petiot, E., Cheval, L., Faugeroux, J., Malard, T., Doucet, A., Jeunemaitre, X., and Hadchouel, J. 2012. A new methodology for quantification of alternatively spliced exons reveals a highly tissue-specific expression pattern of WNK1 isoforms. *PLoS One* 7:e37751.
4. Chavez-Canales, M., Zhang, C., Soukaseum, C., Moreno, E., Pacheco-Alvarez, D., Vidal-Petiot, E., Castaneda-Bueno, M., Vazquez, N., Rojas-Vega, L., Meermeier, N.P., et al. 2014. WNK-SPAK-NCC Cascade Revisited: WNK1 Stimulates the Activity of the

Na-Cl Cotransporter via SPAK, an Effect Antagonized by WNK4. *Hypertension* 64:1047-1053.

5. Xu, B., English, J.M., Wilsbacher, J.L., Stippec, S., Goldsmith, E.J., and Cobb, M.H. 2000. WNK1, a novel mammalian serine/threonine protein kinase lacking the catalytic lysine in subdomain II. *J Biol Chem* 275:16795-16801.
6. Subramanya, A.R., Yang, C.L., Zhu, X., and Ellison, D.H. 2006. Dominant-negative regulation of WNK1 by its kidney-specific kinase-defective isoform. *Am J Physiol Renal Physiol* 290:F619-624.
7. Abriel, H., Loffing, J., Rebhun, J.F., Pratt, J.H., Schild, L., Horisberger, J.D., Rotin, D., and Staub, O. 1999. Defective regulation of the epithelial Na+ channel by Nedd4 in Liddle's syndrome. *J Clin Invest* 103:667-673.
8. Roy, A., Goodman, J.H., Begum, G., Donnelly, B.F., Pittman, G., Weinman, E.J., Sun, D., and Subramanya, A.R. 2015. Generation of WNK1 knockout cell lines by CRISPR/Cas-mediated genome editing. *Am J Physiol Renal Physiol* 308:F366-376.
9. Subramanya, A.R., Liu, J., Ellison, D.H., Wade, J.B., and Welling, P.A. 2009. WNK4 diverts the thiazide-sensitive NaCl cotransporter to the lysosome and stimulates AP-3 interaction. *J Biol Chem* 284:18471-18480.
10. Bostanjoglo, M., Reeves, W.B., Reilly, R.F., Velazquez, H., Robertson, N., Litwack, G., Morsing, P., Dorup, J., Bachmann, S., and Ellison, D.H. 1998. 11Beta-hydroxysteroid dehydrogenase, mineralocorticoid receptor, and thiazide-sensitive Na-Cl cotransporter expression by distal tubules. *J Am Soc Nephrol* 9:1347-1358.
11. McCormick, J.A., Nelson, J.H., Yang, C.L., Curry, J.N., and Ellison, D.H. 2011. Overexpression of the sodium chloride cotransporter is not sufficient to cause familial hyperkalemic hypertension. *Hypertension* 58:888-894.
12. Coleman, R.A., Wu, D.C., Liu, J., and Wade, J.B. 2000. Expression of aquaporins in the renal connecting tubule. *Am J Physiol Renal Physiol* 279:F874-883.
13. Needham, P.G., Mikoluk, K., Dhakarwal, P., Khadem, S., Snyder, A.C., Subramanya, A.R., and Brodsky, J.L. 2011. The thiazide-sensitive NaCl cotransporter is targeted for chaperone-dependent endoplasmic reticulum-associated degradation. *J Biol Chem* 286:43611-43621.
14. Ronzaud, C., Loffing-Cueni, D., Hausel, P., Debonneville, A., Malsure, S.R., Fowler-Jaeger, N., Boase, N.A., Perrier, R., Maillard, M., Yang, B., et al. 2013. Renal tubular NEDD4-2 deficiency causes NCC-mediated salt-dependent hypertension. *J Clin Invest* 123:657-665.